

# Study of $\bar{\Lambda}$ decay parameter in $J/\psi \rightarrow \Lambda \bar{\Lambda}$ decay<sup>\*</sup>

ZHONG Bin(钟彬)<sup>1;2;1)</sup> PING Rong-Gang(平荣刚)<sup>2</sup> XIAO Zhen-Jun(肖振军)<sup>1</sup>

<sup>1</sup> (Department of Physics and Institute of Theoretical Physics, Nanjing Normal University, Nanjing 210097, China)

<sup>2</sup> (Institute of High Energy Physics, CAS, P.O.Box 918(4), Beijing 100049, China)

**Abstract** The helicity amplitudes for  $J/\psi \rightarrow \Lambda \bar{\Lambda}$  and the relevant background decays are presented for measuring the  $\bar{\Lambda}$  decay parameter  $\alpha_+(\bar{\Lambda} \rightarrow \bar{p}\pi^+)$  in  $J/\psi \rightarrow \Lambda \bar{\Lambda}$ . The Monte Carlo (MC) simulations based on the helicity amplitudes information are carried out. The likelihood fit method to determine the  $\bar{\Lambda}$  decay parameter is presented. Based on the MC generated sample, the sensitivity of the measurement for  $\alpha_+$  has been estimated, which shows that the  $J/\psi \rightarrow \Lambda \bar{\Lambda}$  channel can be used to measure the  $\bar{\Lambda}$  decay parameter  $\alpha_+(\bar{\Lambda} \rightarrow \bar{p}\pi^+)$  well.

**Key words** parity asymmetry, hyperon nonleptonic decays,  $J/\psi$  decays

**PACS** 11.80.Cr, 13.20.Gd, 14.20.Jn

## 1 Introduction

The nonleptonic decay of hyperon has long been known as an ideal laboratory to study the parity violation<sup>[1]</sup>. To consider a nonleptonic decay of the hyperon  $Y$ , the angular distribution of the decayed particle takes the form of  $\frac{dN}{d\cos\theta} \propto 1 + \alpha \mathbf{P} \cdot \hat{\mathbf{p}}$ , where  $\mathbf{P}$  is the polarization vector of the hyperon, and  $\hat{\mathbf{p}}$  is the unit vector of the out-going momentum for the decayed particle, and  $\alpha$  is one of the hyperon decay parameters, which characterizes the parity violation in the decays. Till now much evidence for the parity violation in the hyperon decays has been established in experiment. For example, the hyperon decay parameters for  $\Lambda$ ,  $\Sigma^+$ ,  $\Omega^-$  and  $\Xi^-$  have been measured with high precision. The particle data group (PDG) respectively quotes their values as  $\alpha(\Lambda \rightarrow p\pi^-) = 0.642 \pm 0.013$ ,  $\alpha(\Sigma^+ \rightarrow p\pi^0) = -0.980_{-0.015}^{+0.017}$  and  $\alpha(\Xi^- \rightarrow \Lambda\pi^-) = -0.458 \pm 0.012$ <sup>[2]</sup>. However, for the anti-hyperon nonleptonic decays, the decay parameters for  $\bar{\Sigma}^-$  and  $\bar{\Xi}^+$  are not measured; though the  $\bar{\Lambda}$  decay parameter has been measured by DM2 collaboration to be  $\alpha(\bar{\Lambda} \rightarrow \bar{p}\pi^+) = -0.63 \pm 0.13$ <sup>[3]</sup>, the uncertainty ( $\sim 21\%$ ) is still large.

The precise measurement of the  $\bar{\Lambda}$  decay parameter plays an important role in  $CP$  test in  $\Lambda$

decays<sup>[4, 5]</sup>. Under  $CP$  transformation, the decay parameter satisfies  $\alpha_\Lambda = -\alpha_{\bar{\Lambda}}$  if  $CP$  is conserved. If  $CP$ -odd observable is defined by  $A_\Lambda = \frac{\alpha_\Lambda + \alpha_{\bar{\Lambda}}}{\alpha_\Lambda - \alpha_{\bar{\Lambda}}}$ , then any non-zero value of  $A_\Lambda$  observed implies the evidence for  $CP$  asymmetry in  $\Lambda$  decays. Experimentally, searches for  $CP$  asymmetry in  $\Lambda$  nonleptonic decays have been previously performed at  $p\bar{p}$  colliders by the R608<sup>[6]</sup> and PS185<sup>[7]</sup> collaborations, and at an  $e^+e^-$  collider by DM2 Collaboration<sup>[3]</sup>, but the precision of the measurements is limited by statistics.

The precise measurement of the  $\bar{\Lambda}$  decay parameter also plays an important role in the determination of  $\bar{\Omega}^+$  and  $\bar{\Xi}^+$  decay parameters. To note that the non-polarized  $\bar{\Omega}^+$  or  $\bar{\Xi}^+$  decays can produce polarized  $\bar{\Lambda}$  particles. So in the  $\bar{\Lambda}$  rest frame, the angular distribution of the decayed particle, e.g. antiproton, takes the form of  $\frac{dN}{d\cos\theta} \propto 1 + \alpha_{\bar{\Omega}(\bar{\Xi})} \alpha_{\bar{\Lambda}} \cos\theta$ . Experimentally, the extraction of  $\alpha_{\bar{\Omega}(\bar{\Xi})}$  from the product  $\alpha_{\bar{\Omega}(\bar{\Xi})} \alpha_{\bar{\Lambda}}$  is dependent on the value of  $\alpha_{\bar{\Lambda}}$ . Namely, the accuracy of  $\alpha_{\bar{\Omega}}$  or  $\alpha_{\bar{\Xi}}$  measurement is dependent on the uncertainty of  $\alpha_{\bar{\Lambda}}$ .

The decay of  $J/\psi \rightarrow \Lambda \bar{\Lambda}$  is a special place to study the  $\bar{\Lambda}$  decay parameters. Though the produced  $\bar{\Lambda}$  particles are non-polarized, the  $\bar{\Lambda}$  decay parameters can be determined by observation of the helicity correlation between the  $\Lambda$  and  $\bar{\Lambda}$ . Experimentally, this de-

Received 3 December 2007, Revised 12 March 2008

<sup>\*</sup> Supported by National Natural Science Foundation of China (10491303, 10521003) and Knowledge Innovation Project of Chinese Academy of Sciences (U-612 IHEP)

1) E-mail: zhongb@mail.ihep.ac.cn

cay is very clean and easily reconstructed with high efficiency by selecting four charged tracks, and the  $\Lambda/\bar{\Lambda}$  decay length can be used to control the background. Furthermore, this decay allows us to measure  $\alpha(\bar{\Lambda} \rightarrow \bar{n}\pi^0)$  by reconstructing  $\bar{\Lambda}$  with  $\bar{\Lambda} \rightarrow \bar{n}\pi^0$ . For 58 million  $J/\psi$  events collected by BES II detector, we estimate the measurement sensitivity for  $\alpha(\bar{\Lambda} \rightarrow \bar{p}\pi^+)$  to be about 9%. If  $10^{10}$   $J/\psi$  decays are accumulated by BESIII detector, about a few million  $\bar{\Lambda}$  decays will be available, and high accuracy of  $\alpha(\bar{\Lambda} \rightarrow \bar{p}\pi^+)$  achieved.

In Section 2, we present the helicity amplitude formulae for  $J/\psi \rightarrow \Lambda \bar{\Lambda} \rightarrow p\pi^-\bar{p}\pi^+$  and the main backgrounds, including  $J/\psi \rightarrow \Sigma^0\bar{\Sigma}^0 \rightarrow 2\gamma\Lambda\bar{\Lambda} \rightarrow 2\gamma p\pi^-\bar{p}\pi^+$ ,  $J/\psi \rightarrow \Lambda\bar{\Sigma}^0 \rightarrow \gamma\Lambda\bar{\Lambda} \rightarrow \gamma p\pi^-\bar{p}\pi^+$  and  $J/\psi \rightarrow \bar{\Lambda}\Sigma^0 \rightarrow \gamma\Lambda\bar{\Lambda} \rightarrow \gamma p\pi^-\bar{p}\pi^+$ . In Section 3, we introduce the unbinned maximum likelihood method to determine  $\alpha(\bar{\Lambda} \rightarrow \bar{p}\pi^+)$ , do the input output checking, and estimate the sensitivity of the measurement for the parameter  $\alpha(\bar{\Lambda} \rightarrow \bar{p}\pi^+)$ .

## 2 Helicity amplitude analysis

### 2.1 Amplitude for $J/\psi \rightarrow \Lambda \bar{\Lambda}$

The construction of the helicity amplitude is carried out in the helicity frame as shown in Fig. 1. For  $J/\psi \rightarrow \Lambda \bar{\Lambda}$ , the  $z$ -axis of the  $J/\psi$  rest frame is along the  $\Lambda(\bar{\Lambda})$  out-going direction, the solid angle  $(\theta, \phi)$  is between the  $e^+$  direction and the  $\Lambda$  out-going direction; in  $\Lambda(\bar{\Lambda}) \rightarrow p\pi^-(\bar{p}\pi^+)$ , the solid angle of the daughter particle  $\Omega_i(\theta_i, \phi_i)$  is referred to the  $\Lambda(\bar{\Lambda})$  rest frame, the  $z$ -axis is also the  $\Lambda(\bar{\Lambda})$  out-going direction.

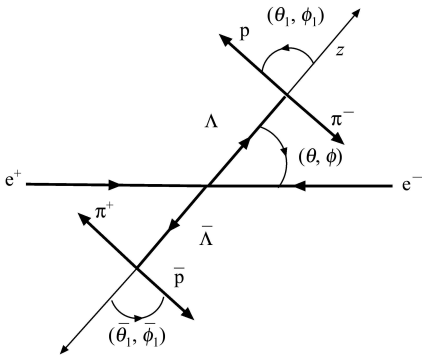


Fig. 1. Definition of the helicity frame for  $J/\psi \rightarrow \Lambda \bar{\Lambda} \rightarrow p\pi^-\bar{p}\pi^+$ .

For  $J/\psi \rightarrow \Lambda \bar{\Lambda} \rightarrow p\pi^-\bar{p}\pi^+$  the joint helicity amplitude can be expressed by  $A_{\lambda, \bar{\lambda}}$  and  $B_{\lambda_p}(\bar{B}_{\lambda_{\bar{p}}})$  as<sup>[8]</sup>:

$$|\mathcal{M}|^2 \propto \sum_{\lambda_1, \bar{\lambda}_1, \lambda_2, \bar{\lambda}_2, \lambda_p, \bar{\lambda}_{\bar{p}}} \rho^{(\lambda_1 - \bar{\lambda}_1, \lambda_2 - \bar{\lambda}_2)}(\theta, \phi) \times A_{\lambda_1, \bar{\lambda}_1} A_{\lambda_2, \bar{\lambda}_2}^* B_{\lambda_p} B_{\lambda_{\bar{p}}}^* \bar{B}_{\lambda_p} \bar{B}_{\lambda_{\bar{p}}}^* \times D_{\lambda_1, \lambda_p}^{1/2*}(\Omega_1) D_{\lambda_2, \lambda_{\bar{p}}}^{1/2}(\Omega_1) \times D_{\lambda_1, \lambda_{\bar{p}}}^{1/2*}(\bar{\Omega}_1) D_{\lambda_2, \bar{\lambda}_{\bar{p}}}^{1/2}(\bar{\Omega}_1), \quad (1)$$

where  $\lambda, \bar{\lambda}$  and  $\lambda_p(\bar{\lambda}_{\bar{p}})$  are the helicity values for  $\Lambda, \bar{\Lambda}$  and proton (antiproton).

$D_{\lambda_1, \lambda_2}^J(\Omega_i) \equiv D_{\lambda_1, \lambda_2}^J(\phi_i, \theta_i, 0)$ , and  $\rho^{(i,j)}(\theta, \phi) = \sum_{k=k \pm 1} D_{i,k}^1(\Omega) D_{j,k}^{1*}(\Omega)$  is the density matrix for the  $J/\psi$  produced in  $e^+e^-$  annihilation. From parity invariance, one has  $A_{-\lambda_1, -\lambda_2} = A_{\lambda_1, \lambda_2}$ . The asymmetry parameters in  $\Lambda(\bar{\Lambda})$  decays are defined as:

$$\alpha_\Lambda = \frac{|B_{1/2}|^2 - |B_{-1/2}|^2}{|B_{1/2}|^2 + |B_{-1/2}|^2}, \quad \alpha_{\bar{\Lambda}} = \frac{|\bar{B}_{1/2}|^2 - |\bar{B}_{-1/2}|^2}{|\bar{B}_{1/2}|^2 + |\bar{B}_{-1/2}|^2}. \quad (2)$$

If  $CP$  invariance is conserved, one has  $B_\lambda = -\bar{B}_{-\lambda}$ . This leads to  $\alpha_\Lambda = -\alpha_{\bar{\Lambda}}$ . After integrating over  $\phi$ , Eq. (1) is simplified as:

$$\frac{d|\mathcal{M}|^2}{d(\cos\theta)d\Omega_1d\bar{\Omega}_1} \propto 4|A_{1/2,1/2}|^2 \sin^2\theta \times [1 + \alpha_\Lambda \alpha_{\bar{\Lambda}} (\cos\theta_1 \cos\bar{\theta}_1 + \sin\theta_1 \sin\bar{\theta}_1 \cos(\phi_1 + \bar{\phi}_1))] - 2|A_{1/2,-1/2}|^2 (1 + \cos^2\theta) (\alpha_\Lambda \alpha_{\bar{\Lambda}} \cos\theta_1 \cos\bar{\theta}_1 - 1). \quad (3)$$

After further integrating over the solid angles  $\Omega_1$  and  $\bar{\Omega}_1$ , as expected, the above equation is reduced to the well known formula:

$$\frac{d|\mathcal{M}|^2}{d\cos\theta} \propto (1 + \alpha \cos^2\theta), \quad \text{with} \quad \alpha = \frac{|A_{1/2,-1/2}|^2 - 2|A_{1/2,1/2}|^2}{|A_{1/2,-1/2}|^2 + 2|A_{1/2,1/2}|^2}, \quad (4)$$

where  $\alpha$  is the angular distribution parameter for  $J/\psi \rightarrow \Lambda \bar{\Lambda}$ , which is recently measured by BES II to be  $\alpha = 0.65 \pm 0.11$ <sup>[9]</sup>. From Eq. (4), if the normalization condition is selected as  $|A_{1/2,-1/2}|^2 + 2|A_{1/2,1/2}|^2 = 1$ , one has:

$$|A_{1/2,-1/2}|^2 = \frac{1+\alpha}{2} \quad \text{and} \quad |A_{1/2,1/2}|^2 = \frac{1-\alpha}{4}. \quad (5)$$

Combining Eq. (3) and Eq. (5), one gets:

$$\frac{d|\mathcal{M}|^2}{d(\cos\theta)d\Omega_1d\bar{\Omega}_1} \propto (1-\alpha) \sin^2\theta \times [1 + \alpha_\Lambda \alpha_{\bar{\Lambda}} (\cos\theta_1 \cos\bar{\theta}_1 + \sin\theta_1 \sin\bar{\theta}_1 \cos(\phi_1 + \bar{\phi}_1))] - (1+\alpha)(1 + \cos^2\theta) (\alpha_\Lambda \alpha_{\bar{\Lambda}} \cos\theta_1 \cos\bar{\theta}_1 - 1). \quad (6)$$

Eq. (6) is our master equation to fit to the data

to determine  $\alpha_{\bar{\Lambda}}$  by fixing  $\alpha_{\Lambda} = 0.642$ . It is also used for the Monte Carlo generation of  $J/\psi \rightarrow \Lambda\bar{\Lambda}$ .

## 2.2 Amplitudes for background channels

Although the signal of  $J/\psi \rightarrow \Lambda\bar{\Lambda} \rightarrow p\pi^-\bar{p}\pi^+$  is very clean (the contamination of background events is less than 5%), it still needs to receive a proper treatment for determining the  $\bar{\Lambda}$  decay parameter. Especially for the backgrounds including the  $\bar{\Lambda}$  decays, their effects on the extraction of the  $\bar{\Lambda}$  decay parameter should be under full study with MC simulations. By running the inclusive  $J/\psi$  MC sample, it is found that there are two dominant background channels including  $\bar{\Lambda}$  decays:  $J/\psi \rightarrow \Sigma^0\bar{\Sigma}^0 \rightarrow 2\gamma\Lambda\bar{\Lambda} \rightarrow 2\gamma p\pi^-\bar{p}\pi^+$ , and  $J/\psi \rightarrow \Lambda\bar{\Sigma}^0 + c.c. \rightarrow \gamma\Lambda\bar{\Lambda} \rightarrow \gamma p\pi^-\bar{p}\pi^+$ . Although the second decay is the isospin violation process, the branching fraction is not negligible. The PDG quotes  $Br(J/\psi \rightarrow \Lambda\bar{\Sigma} + c.c.) < 1.5 \times 10^{-4}$  at 90% confidence level. We simulate these channels using helicity amplitude information. Similar to the previous case, the helicity amplitudes are constructed as follows.

### 2.2.1 $J/\psi \rightarrow \Sigma^0\bar{\Sigma}^0 \rightarrow 2\gamma\Lambda\bar{\Lambda} \rightarrow 2\gamma p\pi^-\bar{p}\pi^+$

Under the similar definition for the helicity frame, the helicity amplitude reads<sup>[8]</sup>:

$$|\mathcal{M}|^2 = \sum_{\substack{\sigma_1, \sigma_2, \bar{\sigma}_1, \bar{\sigma}_2, \\ \lambda_1, \lambda_2, \bar{\lambda}_1, \bar{\lambda}_2, \\ r_1, r_2, \lambda_p, \lambda_{\bar{p}}}} \rho^{(\sigma_1 - \bar{\sigma}_1, \sigma_2 - \bar{\sigma}_2)}(\theta, \phi) A_{\sigma_1, \bar{\sigma}_1} A_{\sigma_2, \bar{\sigma}_2}^* \times \\ B_{r_1, \lambda_1} B_{r_1, \lambda_2}^* C_{\lambda_p} C_{\lambda_{\bar{p}}}^* \bar{B}_{r_2, \bar{\lambda}_1} \bar{B}_{r_2, \bar{\lambda}_2}^* \bar{C}_{\lambda_{\bar{p}}} \bar{C}_{\lambda_p}^* \times \\ D_{\sigma_1, r_1 - \lambda_1}^{1/2 *}(\Omega_1) D_{\sigma_2, r_1 - \lambda_2}^{1/2}(\Omega_1) \times \\ D_{\bar{\sigma}_1, r_2 - \bar{\lambda}_1}^{1/2 *}(\bar{\Omega}_1) D_{\bar{\sigma}_2, r_2 - \bar{\lambda}_2}^{1/2}(\bar{\Omega}_1) \times \\ D_{\lambda_1, \lambda_p}^{1/2 *}(\Omega_2) D_{\lambda_2, \lambda_{\bar{p}}}^{1/2}(\Omega_2) \times \\ D_{\bar{\lambda}_1, \lambda_{\bar{p}}}^{1/2 *}(\bar{\Omega}_2) D_{\bar{\lambda}_2, \lambda_p}^{1/2}(\bar{\Omega}_2), \quad (7)$$

where  $A_{\sigma, \bar{\sigma}}$ ,  $B_{\lambda}$  and  $C_{\lambda_p}$  denote the helicity amplitude for  $J/\psi \rightarrow \Sigma^0(\sigma)\bar{\Sigma}^0(\bar{\sigma})$ ,  $\Sigma^0(\sigma) \rightarrow \gamma(r_1)\Lambda(\lambda)$  and  $\Lambda(\lambda) \rightarrow p(\lambda_p)\pi^-$  separately. To consider the parity invariance in  $J/\psi \rightarrow \Sigma^0\bar{\Sigma}^0$  and  $\Sigma^0 \rightarrow \gamma\Lambda$ , one has  $A_{-\sigma_1, -\sigma_2} = A_{\sigma_1, \sigma_2}$ ,  $B_{-r, -\lambda} = B_{r, \lambda}$  and  $\bar{B}_{-r, -\lambda} = \bar{B}_{r, \lambda}$ . By integrating the azimuthal angles  $\phi$ ,  $\phi_1$  and  $\bar{\phi}_1$ , one gets:

$$\frac{d|\mathcal{M}|^2}{d\cos\theta d\Omega_1 d\bar{\Omega}_1 d\cos\theta_2 d\cos\bar{\theta}_2} \propto \\ |B_{1,1/2}|^2 |\bar{B}_{1,1/2}|^2 \{4\sin^2\theta [\cos\theta_2 \cos\bar{\theta}_2 (\cos\theta_1 \times \\ \cos\bar{\theta}_1 \cos(\phi_1 + \bar{\phi}_1) \sin\theta_1 \sin\bar{\theta}_1) \alpha_{\Lambda} \alpha_{\bar{\Lambda}} + 1] \times \\ |A_{1/2,1/2}|^2 - (\cos 2\theta + 3)(\cos\theta_1 \cos\theta_2 \cos\bar{\theta}_1 \times \\ \cos\bar{\theta}_2 \alpha_{\Lambda} \alpha_{\bar{\Lambda}} - 1) |A_{1/2,-1/2}|^2\}. \quad (8)$$

Combining Eq. (5), one gets:

$$\frac{d|\mathcal{M}|^2}{d\cos\theta d\Omega_1 d\bar{\Omega}_1 d\cos\theta_2 d\cos\bar{\theta}_2} \propto \\ |B_{1,1/2}|^2 |\bar{B}_{1,1/2}|^2 \{ (1 - \alpha) \sin^2\theta [\cos\theta_2 \cos\bar{\theta}_2 (\cos\theta_1 \times \\ \cos\bar{\theta}_1 + \cos(\phi_1 + \bar{\phi}_1) \sin\theta_1 \sin\bar{\theta}_1) \alpha_{\Lambda} \alpha_{\bar{\Lambda}} + 1] - \\ \left(\frac{1 + \alpha}{2}\right) (\cos 2\theta + 3) (\cos\theta_1 \cos\theta_2 \times \\ \cos\bar{\theta}_1 \cos\bar{\theta}_2 \alpha_{\Lambda} \alpha_{\bar{\Lambda}} - 1) \}. \quad (9)$$

### 2.2.2 $J/\psi \rightarrow \Lambda\bar{\Sigma}^0 + c.c. \rightarrow \gamma\Lambda\bar{\Lambda} \rightarrow \gamma p\pi^-\bar{p}\pi^+$

These two decays are conjugated channels; their helicity amplitudes have the similar structure. The helicity amplitude reads:

$$|\mathcal{M}|^2 = \sum_{\substack{\sigma, \lambda, \sigma', \lambda', \\ \lambda_p, \lambda_{\bar{p}}, r, \lambda, \lambda'}} \rho^{(\lambda - \sigma, \lambda' - \sigma')}(\Omega_0) \times \\ A_{\lambda, \sigma} A_{\lambda', \sigma'}^* B_{\lambda_p} B_{\lambda_{\bar{p}}}^* C_{r, \bar{\lambda}} C_{r, \bar{\lambda}'}^* D_{\lambda_{\bar{p}}} D_{\lambda_p}^* \times \\ D_{\lambda, \lambda_p}^{1/2 *}(\Omega_1) D_{\lambda', \lambda_{\bar{p}}}^{1/2}(\Omega_1) \times \\ D_{\sigma, r - \bar{\lambda}}^{1/2 *}(\Omega_2) D_{\sigma', r - \bar{\lambda}'}^{1/2}(\Omega_2) \times \\ D_{\bar{\lambda}, \lambda_{\bar{p}}}^{1/2 *}(\Omega_3) D_{\bar{\lambda}', \lambda_p}^{1/2}(\Omega_3), \quad (10)$$

where  $A_{\lambda, \sigma}$ ,  $B_{\lambda_p}$ ,  $C_{r, \bar{\lambda}}$  and  $D_{\lambda_{\bar{p}}}$  denote the helicity amplitude for  $J/\psi \rightarrow \Lambda\bar{\Sigma}^0(\Omega_0)$ ,  $\Lambda \rightarrow p\pi^-(\Omega_1)$ ,  $\bar{\Sigma}^0 \rightarrow \gamma\bar{\Lambda}(\Omega_2)$  and  $\bar{\Lambda} \rightarrow \bar{p}\pi^+$ , respectively. By integrating the azimuthal angle  $\phi_0$ , one has:

$$\frac{d|\mathcal{M}|^2}{d\cos\theta_0 d\Omega_1 d\Omega_2 d\Omega_3} \propto \\ 4\sin^2\theta_0 [\cos\theta_3 (\cos\theta_1 \cos\theta_2 + \cos(\phi_1 + \phi_2)) \times \\ \sin\theta_1 \sin\theta_2) \alpha_{\Lambda} \alpha_{\bar{\Lambda}} + 1] |A_{1/2,1/2}|^2 - \\ (\cos 2\theta_0 + 3) (\cos\theta_1 \cos\theta_2 \cos\theta_3 \times \\ \alpha_{\Lambda} \alpha_{\bar{\Lambda}} - 1) |A_{1/2,-1/2}|^2. \quad (11)$$

Combining Eq. (5), one gets:

$$\frac{d|\mathcal{M}|^2}{d\cos\theta_0 d\Omega_1 d\Omega_2 d\Omega_3} \propto \\ (1 - \alpha) \sin^2\theta_0 [\cos\theta_3 (\cos\theta_1 \cos\theta_2 + \cos(\phi_1 + \phi_2)) \times \\ \sin\theta_1 \sin\theta_2) \alpha_{\Lambda} \alpha_{\bar{\Lambda}} + 1] - \\ \left(\frac{1 + \alpha}{2}\right) (\cos 2\theta_0 + 3) \times \\ (\cos\theta_1 \cos\theta_2 \cos\theta_3 \alpha_{\Lambda} \alpha_{\bar{\Lambda}} - 1). \quad (12)$$

## 3 Monte-Carlo simulation

### 3.1 Event generation and selection

The decay events are generated with the full helicity amplitude information as obtained above. The

parameters in the amplitudes are fixed at the existing measured values. For example, the signal event  $J/\psi \rightarrow \Lambda \bar{\Lambda} \rightarrow p\pi^- \bar{p}\pi^+$  is dynamically generated by making use of Eq. (6), and the angular distribution parameter  $\alpha$  is fixed at 0.62, the asymmetry parameter  $\alpha_{\Lambda}\alpha_{\bar{\Lambda}}$  is fixed at  $-0.412$ , which quotes PDG value  $\alpha_{\Lambda} = -\alpha_{\bar{\Lambda}} = 0.642$ ; For background decays,  $J/\psi \rightarrow \Sigma^0 \bar{\Sigma}^0 \rightarrow 2\gamma\Lambda\bar{\Lambda} \rightarrow 2\gamma p\pi^- \bar{p}\pi^+$ , is generated according to Eq. (9), in which the angular distribution parameter  $\alpha$  is fixed at  $-0.24$ <sup>[9]</sup>, and the asymmetry parameter  $\alpha_{\Lambda}\alpha_{\bar{\Lambda}}$  is fixed at  $-0.412$ ; The decays  $J/\psi \rightarrow \Lambda \bar{\Sigma}^0 \rightarrow \gamma\Lambda\bar{\Lambda} \rightarrow \gamma p\pi^- \bar{p}\pi^+$  and its conjugate decays  $J/\psi \rightarrow \bar{\Lambda}\Sigma^0 \rightarrow \gamma\Lambda\bar{\Lambda} \rightarrow \gamma p\pi^- \bar{p}\pi^+$  are generated with Eq. (12), where the angular distribution  $\alpha$  is fixed at  $0.25$ <sup>[10]</sup>, the asymmetry parameter  $\alpha_{\Lambda}\alpha_{\bar{\Lambda}}$  is fixed at  $-0.412$ .

The number of the generated background samples is listed in Table 1. The event construction is carried out by using strict event selection rules. The signal events are required to have exact four reconstructed charged tracks in the drift chamber with to-

tal zero net charge, the detector reception coverage is  $|\cos\theta| < 0.8$  (where  $\theta$  is the polar angle for tracks), the transverse momentum  $p_{xy}$  is greater than  $0.07 \text{ GeV}/c$ , the kinematic fit  $\chi^2$  is less than 16, the  $\Lambda$  and  $\bar{\Lambda}$  invariant mass satisfy  $|M_{p\pi^-} - 1.1156| < 0.0255$  and  $|M_{\bar{p}\pi^+} - 1.1156| < 0.0255$ , respectively. Under these cuts, the efficiency of the signal channel  $J/\psi \rightarrow \Lambda \bar{\Lambda}$  is about 20%, the survived events are about 10000.

The contamination from the background decays estimated with the generated background samples is also listed in Table 1. The background decays are also required to pass through the cuts used for signal event selection. The survived background events for the three channels are normalized according to the  $58 \times 10^6$   $J/\psi$  data sample and each branching fractions, respectively. These total normalized background events are less than 100. Compared with the survived signal events, the background events are few, which indicates the selection of the signal  $J/\psi \rightarrow \Lambda \bar{\Lambda}$  is very clean.

Table 1. The background samples.

channel	generated events	survived events	branching ratio	normalization*
$J/\psi \rightarrow \Sigma^0 \bar{\Sigma}^0$	$1 \times 10^5$	25	$1.31 \times 10^{-3}$	19
$J/\psi \rightarrow \Lambda \bar{\Sigma}^0$	$1 \times 10^5$	669	$< 0.75 \times 10^{-4}$	$< 29$
$J/\psi \rightarrow \bar{\Lambda} \Sigma^0$	$1 \times 10^5$	656	$< 0.75 \times 10^{-4}$	$< 29$

\* The numbers in last column are normalized to 58 M  $J/\psi$  events collected by BES II detector.

### 3.2 Input output checking

We use the unbinned maximum likelihood method to determine the  $\bar{\Lambda}$  asymmetric parameter, and then do the input output checking and the sensitivity estimation. The joint likelihood is defined by:

$$\mathcal{L} = \prod_{i=1}^N \text{Prob}(p_i) = \prod_{i=1}^N \frac{|\mathcal{M}(p_i)|^2 \epsilon(p_i)}{\int dp_i |\mathcal{M}(p_i)|^2 \epsilon(p_i)}, \quad (13)$$

where  $\text{Prob}(p_i)$  is the probability to produce event  $i$  characterized by the measurements  $p_i$ ,  $\mathcal{M}_{p_i}$  is the amplitude of event  $i$ . To determine the parameters in question, we have to minimize the objective function defined by

$$\mathcal{S} = -\ln \mathcal{L} = -\sum_{i=1}^N \ln \left[ \frac{|\mathcal{M}(p_i)|^2}{\int dp_i |\mathcal{M}(p_i)|^2 \epsilon(p_i)} \right]. \quad (14)$$

In the above equation, the term  $\ln \epsilon(p_i)$  is neglected because the detection efficiency  $\epsilon(p_i)$  is independent on the determination of  $\bar{\Lambda}$  decay parameters. If the generated events are not required to pass through the detector simulation, then  $\epsilon(p_i) = 1$ .

The input output checking is used to test the fit-

ting procedure. The generated Monte Carlo sample of  $J/\psi \rightarrow \Lambda \bar{\Lambda}$  is to do the work. The fitting results are given in Fig. 2. It can be seen that the output values determined by the likelihood fit method vary little with the event number  $N$ . All the output values are in good agreement with the input values. The precision of about 95% is achieved, indicating the validity of the fitting procedure.

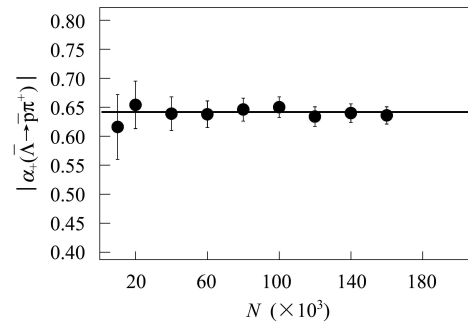


Fig. 2. The input output checking varies with the event number  $N$  for determining  $\alpha_+(\bar{\Lambda} \rightarrow \bar{p}\pi^+)$  in  $J/\psi \rightarrow \Lambda \bar{\Lambda}$ . The dots with error bar are the output values determined with the likelihood fit method, and the solid line is the input value.

### 3.3 Sensitivity estimation

Experimentally, the sensitivity of the measurement for a parameter  $\alpha$  is defined by

$$\delta(\alpha) = \frac{\sqrt{V(\alpha)}}{\alpha}, \quad (15)$$

$$\delta(\alpha_{\bar{\Lambda}}) \approx \frac{1}{\alpha_{\bar{\Lambda}}} \sqrt{\frac{9(d-2)^2(d+1)\sqrt{d^2-4}}{N \left\{ 48d^2i \tanh^{-1} \left( \sqrt{\frac{2-d}{2+d}} \right) + (d+2)[(d-9)d+2]\sqrt{d^2-4} \right\}}} \quad \text{with } d = \frac{2(1+\alpha)}{1-\alpha}, \quad (16)$$

Table 2. Evaluation of sensitivity by numerical calculation. The efficiency quotes the result of Monte Carlo simulation. The measured  $\alpha(\bar{\Lambda} \rightarrow \bar{p}\pi^+)$  quotes  $-0.642 \pm 0.013$ .

channel	efficiency	parameter	sensitivity $\delta(\alpha)$
$J/\psi \rightarrow \Lambda\bar{\Lambda}$ (BES II)	$\epsilon = 20\%$	$\alpha_+(\bar{\Lambda} \rightarrow \bar{p}\pi^+)$	$\sim 9 \times 10^{-2}$
$J/\psi \rightarrow \Lambda\bar{\Lambda}$ (BES III)	$\epsilon = 20\%$ at least	$\alpha_+(\bar{\Lambda} \rightarrow \bar{p}\pi^+)$	$\sim 3 \times 10^{-3}$

where  $N$  is the number of observed events, and  $\alpha$  is the angular distribution parameter defined in Eq. (4).

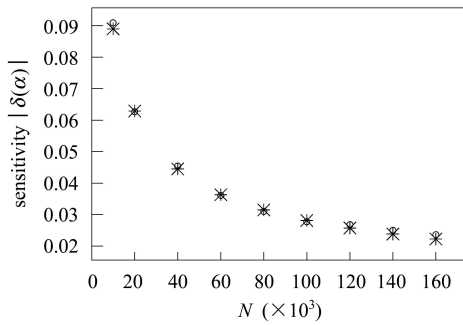


Fig. 3. The measurement sensitivity varies with the event number  $N$  for determining  $\alpha_+(\bar{\Lambda} \rightarrow \bar{p}\pi^+)$  in  $J/\psi \rightarrow \Lambda\bar{\Lambda}$ . The circles are the sensitivities determined with the likelihood fit method, and the stars are the numerical results calculated with Eq. (15).

The same sample which is used to do the input output checking is also used to carry out the sensitivity estimation. The results and the comparison with the theoretical evaluation are given in Fig. 3. It can be seen that the sensitivity values are in good agreement with those obtained from the numerical calculation by Eq. (15). For the sample of  $58 \times 10^6$   $J/\psi$  events collected by BES II detector, the selected

where  $V(\alpha)$  is the variance of parameter  $\alpha$ . With the joint angular distribution, the evaluation of sensitivity is straightforward by using the maximum likelihood method as shown in Ref. [11]. For the measurement of  $\alpha_{\bar{\Lambda}}$  in  $J/\psi \rightarrow \Lambda\bar{\Lambda} \rightarrow p\pi^-\bar{p}\pi^+$ , the sensitivity reads<sup>[8]</sup>:

$J/\psi \rightarrow \Lambda\bar{\Lambda}$  events are about  $1 \times 10^4$  if the detection efficiency is taken as 20%, then the sensitivity to measure  $\alpha_+(\bar{\Lambda} \rightarrow \bar{p}\pi^+)$  is about 9%, which is improved as twice as the existing result (21%). If the BES III detector collects a sample of  $10^{10}$   $J/\psi$  events, the sensitivity of about  $3 \times 10^{-3}$  will be achieved in the near future. The results are listed in Table 2. It is clear as listed that the decay  $J/\psi \rightarrow \Lambda\bar{\Lambda}$  is the most potential channel used to measure the  $\bar{\Lambda}$  decay parameter.

## 4 Summary

The helicity amplitudes for  $J/\psi \rightarrow \Lambda\bar{\Lambda} \rightarrow p\pi^-\bar{p}\pi^+$ ,  $J/\psi \rightarrow \Sigma^0\bar{\Sigma}^0 \rightarrow 2\gamma\Lambda\bar{\Lambda} \rightarrow 2\gamma p\pi^-\bar{p}\pi^+$ ,  $J/\psi \rightarrow \Lambda\bar{\Sigma}^0 \rightarrow \gamma\Lambda\bar{\Lambda} \rightarrow \gamma p\pi^-\bar{p}\pi^+$  and  $J/\psi \rightarrow \bar{\Lambda}\Sigma^0 \rightarrow \gamma\Lambda\bar{\Lambda} \rightarrow \gamma p\pi^-\bar{p}\pi^+$  are presented for studying the  $\bar{\Lambda}$  decay parameter  $\alpha_+(\bar{\Lambda} \rightarrow \bar{p}\pi^+)$  in  $J/\psi \rightarrow \Lambda\bar{\Lambda}$ . The Monte Carlo simulations based on the helicity amplitudes information are carried out. The results show that the background contamination in the signal event selection of  $J/\psi \rightarrow \Lambda\bar{\Lambda}$  is low. The likelihood fit method to determine the  $\bar{\Lambda}$  decay parameter is presented. Based on the MC generated sample, the estimations of the sensitivity would be 9% and  $3 \times 10^{-3}$  for BES II and BES III measurements, respectively. This indicates that the decay  $J/\psi \rightarrow \Lambda\bar{\Lambda}$  is the potential channel used to measure the  $\bar{\Lambda}$  decay parameter  $\alpha_+(\bar{\Lambda} \rightarrow \bar{p}\pi^+)$ .

## References

- LEE T D, YANG C N. Phys. Rev., 1957, **108**: 1645; LEE T D, Steinberger J, Feinberg G et al. Phys. Rev., 1957, **106**: 1367
- Particle Data Group. J. Phys. G, 2006, **33**: 1
- Tixier M H et al. Phys. Lett. B, 1988, **212**: 523
- CHAN A W et al. Phys. Rev. D, 1988, **58**: 072002
- Pais A. Phys. Rev. Lett., 1959, **3**: 242

- Chauvat P et al. Phys. Lett. B, 1985, **163**: 273
- Barnes P D et al. Phys. Rev. C, 1996, **54**: 1877
- CHEN H, PING R G. Phys. Rev. D, 2007, **76**: 036005
- Ablikim M et al. (BES Collab.). Phys. Lett. B, 2006, **632**: 181
- Korner J G. Z. Phys. C, 1987, **33**: 529
- Meyer Stuart L. Data Analysis for Scientists and Engineers. New York: John Wiley & Sons, 1975. 331